

Resolution of Black Hole Singularities in Jackiw-Teitelboim Gravity

DONGSU BAK,^a CHANJU KIM,^b SANG-HEON YI,^a

a) *Physics Department & Natural Science Research Institute
University of Seoul, Seoul 02504 KOREA*

b) *Department of Physics, Ewha Womans University, Seoul 03760 KOREA*

(dsbak@uos.ac.kr, cjkim@ewha.ac.kr, shyi704@uos.ac.kr)

ABSTRACT

In Jackiw-Teitelboim gravity, the naive Schwarzsian quantum mechanics leads to a continuous bulk spectrum, in apparent contradiction with the finite entropy of the black hole, which requires a discrete spectrum with level spacing of order e^{-S_0} . It was recently shown that restoring spectral discreteness with random statistics requires the introduction of a left confining potential that becomes relevant when the renormalized wormhole length reaches order e^{S_0} . In this work, we show how the known perturbative results of JT gravity are recovered within this modified framework. More importantly, we demonstrate that this modification has a direct dynamical consequence: it resolves the black-hole singularity. The confining potential generates a repulsive force at exponentially large wormhole length, preventing the indefinite growth that would otherwise lead to a singularity. We explain in detail how this turnaround arises and explore its implications for late-time bulk gravitational dynamics, the disappearance of horizons, and possible observational consequences.

1 Introduction

In Jackiw-Teitelboim (JT) gravity [1–3], the vacuum solution describes a Lorentzian two-sided black hole, which corresponds to the disk geometry on the Euclidean side [4]. The Lorentzian spacetime contains a wormhole connecting the left and right asymptotic boundaries, and its renormalized length (or, in higher dimensions, the renormalized volume) provides a gauge-invariant geometric observable [5–10]. Upon quantization, this degree of freedom reduces at leading order to Schwarzian quantum mechanics [11–13], whose wave function depends on the variable $\chi = -\ell_{ren}/2$ with ℓ_{ren} denoting the renormalized wormhole length.

The black hole carries a finite number of degrees of freedom, and therefore its energy spectrum is expected to be discrete, with a typical level spacing of order e^{-S_0} . However, in the Schwarzian description the dynamical variable χ ranges over the entire real line, and the Liouville potential $e^{2\chi}$ is not confining. As a result, the corresponding quantum-mechanical spectrum is continuous [14]. This is in contradiction with the finiteness of the black hole entropy, which demands a discrete spectrum.

In our previous work [15], we resolved this issue by introducing a left confining potential that becomes $O(1)$ only when $\chi = -O(e^{S_0})$. Consequently, the potential effectively disappears in the limit S_0 goes to infinity, which corresponds to the continuum limit familiar from semiclassical gravity. At leading order, the left confining potential $W(X)$, with the rescaled variable $X = -2\chi e^{-S_0}$, is determined explicitly through a semiclassical analysis that reproduces the well-known disk density of states [16, 17]. Higher-order corrections are incorporated by introducing random components into the potential, capturing the subleading effects beyond the semiclassical approximation.

This modification leads to a dramatic change in the gravitational dynamics once the wormhole length reaches $O(e^{S_0})$, an exponentially large scale. The wormhole length can be identified with the so-called Krylov spread complexity [18–23]. For a finite-temperature quantum-mechanical system with a discrete spectrum and random level statistics, it is well known that the Krylov spread complexity initially grows exponentially in time, accompanied by a universal linear growth, reaches a maximum, and then decreases before eventually saturating at a plateau. In this late-time regime, the system becomes effectively maximally random and highly complex (see [24–26] for reviews of Krylov spread complexity).

In this note, we examine the implications of introducing the left confining potential. A particularly striking consequence is the resolution of the black hole singularity. We explain in detail how this resolution arises and discuss its physical implications. In essence, the singularity is resolved because the left confining potential generates a repulsive force that

counteracts the otherwise purely attractive gravitational dynamics. Since this confining potential originates from the discreteness of the energy spectrum, it follows that spectral discreteness itself is ultimately responsible for the singularity resolution. In this sense, the mechanism is intrinsically nonclassical. In the absence of the left confining potential, the linear growth of the wormhole length up to times $t \sim O(e^{S_0})$ would inevitably lead to a singularity. Up to this regime, gravity remains purely attractive and exhibits the familiar features of chaotic dynamics, thermalization, and scrambling on $O(1)$ timescales, reflecting its thermodynamic character. By contrast, the regime near the maximum of the complexity—the top, the subsequent downward slope, and the eventual plateau—corresponds to exponentially long timescales that are usually neglected. It is precisely in this regime that the effects of spectral discreteness become dominant and qualitatively modify the bulk dynamics.

Section 2 reviews JT gravity and explains how the singularity arises in the standard formulation. We also briefly summarize the Saad–Shenker–Stanford (SSS) duality [4]. In Section 3, we introduce the left confining potential on the JT side and explain how the perturbative results are recovered within the modified JT framework. Section 4 demonstrates how the singularity is resolved, while the corresponding bulk interpretation is presented in Section 5. The final section is devoted to conclusions and discussions. In the Appendix, we show how the perturbative genus expansion emerges in our framework and demonstrate explicitly that its first few terms satisfy nontrivial consistency conditions.

2 Bulk singularity from boundary dynamics

We begin this section with the bulk JT gravity action,

$$I = \frac{1}{16\pi G} \int_M d^2x \sqrt{-g} \phi(R + 2) + \frac{1}{8\pi G} \int_{\partial M} dt \sqrt{-\gamma_{tt}} \phi(K - 1), \quad (2.1)$$

where ϕ denotes a dilaton field, t represents the physical boundary time, and γ_{tt} and K are the induced metric and the extrinsic curvature on the boundary ∂M , respectively. In the two-sided Lorentzian setup, the boundary term contains contributions from both the left and right asymptotic boundaries. Varying the action with respect to the dilaton and the metric yields the bulk equations of motion:

$$0 = R + 2, \quad (2.2)$$

$$0 = \nabla_a \nabla_b \phi - g_{ab} \nabla^2 \phi + g_{ab} \phi. \quad (2.3)$$

The first equation dictates the bulk spacetime to be locally AdS₂. In the Euclidean framework, we can also include topological terms,

$$I_E^{\text{top}} = -\frac{S_0}{2\pi} \frac{1}{8\pi G} \left[\frac{1}{2} \int_{M_E} \sqrt{g} R + \int_{\partial M_E} \sqrt{\gamma} K \right], \quad (2.4)$$

which can be used for the natural topological expansion by powers of e^{-S_0} . Below we shall set $8\pi G = 1$ for the simplicity of our presentation.

Now, we briefly review the boundary dynamics of the AdS₂ geometry. We work with the global AdS_2 metric

$$ds^2 = \frac{-d\tau^2 + d\mu^2}{\cos^2 \mu}, \quad (2.5)$$

with $\mu \in [-\pi/2, \pi/2]$ where $\mu = \pm\pi/2$ correspond to the left and right spatial infinities, respectively. The cutoff trajectory is defined by fixing the value of the dilaton as

$$\phi(\tau, \mu)|_c = \frac{\bar{\phi}}{\epsilon}, \quad (2.6)$$

following Refs. [3, 11, 27–30]. The boundary physical time t is determined by requiring that the induced metric on the cutoff trajectory takes the form

$$ds^2|_c = -\frac{dt^2}{\epsilon^2}. \quad (2.7)$$

The left and right cutoff trajectories are determined by embedding functions $\tau = \tau(t)$ and $\mu = \mu_c(t)$. Imposing the induced metric condition yields

$$\cos \mu_c(t) = \epsilon \dot{\tau}, \quad (2.8)$$

where the dot denotes differentiation with respect to the physical boundary time t . Now suppose the dilaton admits the near-boundary expansion

$$\phi = \frac{\bar{\phi}}{\epsilon} \left(\frac{G(\tau)}{\cos \mu} + O(\cos \mu) \right). \quad (2.9)$$

Evaluating this expression on the cutoff trajectories and using condition (2.6), we arrive at the simple boundary relation

$$\dot{\tau} = G(\tau). \quad (2.10)$$

Thus, the boundary time reparametrization is determined directly by the leading near-boundary behavior of the dilaton. This relation encodes how the bulk dilaton profile fixes the boundary dynamics.

With this preparation, the left and right boundary Lagrangians take the Schwarzian form

$$L_{r/l} = -\mathcal{C} \text{Sch} \left(\tan \frac{\tau_{r/l}(t)}{2}, t \right), \quad (2.11)$$

where $\mathcal{C} = \bar{\phi}$ and the Schwarzian derivative is defined by

$$\text{Sch}(f(x), x) = -\frac{1}{2}(f''/f')^2 + (f''/f)'. \quad (2.12)$$

It is convenient to rewrite the Schwarzian action in a first-order form,

$$L_{r/l} = \frac{\mathcal{C}}{2}(\dot{\chi}_{r/l})^2 - \frac{1}{2\mathcal{C}}e^{2\chi_{r/l}} + p_{r/l} \left(\dot{\tau}_{r/l} - \frac{1}{\mathcal{C}}e^{\chi_{r/l}} \right), \quad (2.13)$$

where $p_{r/l}$ plays a role of Lagrange multiplier. After fully fixing the large gauge redundancy and quantizing the constrained system (see, for example, [31] for details), the left and right sectors become identical and the total boundary Lagrangian reduces to

$$L_{total} = L_r + L_l = \mathcal{C}(\dot{\chi})^2 - \frac{1}{\mathcal{C}}e^{2\chi} \quad (2.14)$$

with $\chi = \chi_l = \chi_r$ and $p_\chi/2 = p_{\chi_r} = p_{\chi_l}$. Also note that $H_{total}/2 = H_l = H_r = H$ where H_{total} is the Hamiltonian derived from the above Lagrangian (2.14). In particular, the Hamiltonian H takes the form

$$2\mathcal{C}H = \frac{1}{4}p_\chi^2 + e^{2\chi} = p_q^2 + e^q \quad (2.15)$$

with $q = 2\chi$. The variable χ is defined with the relation $e^\chi = \mathcal{C}\dot{\tau}$ and one can show that the renormalized wormhole length ℓ_{ren} is given by $\ell_{ren} = -2\chi$ [31].

With the relation (2.10), let us compare the resulting equation of motion. First note that $\dot{\chi} = \dot{\tau}G'/G$ with a prime here denoting a τ derivative and, if we use (2.10) again, one has $\dot{\chi} = G'$. With one more t derivative, we are led to

$$\mathcal{C}\ddot{\chi} = \mathcal{C}G''\dot{\tau} = \mathcal{C}GG'' = -\frac{e^{2\chi}}{\mathcal{C}}, \quad (2.16)$$

where we use the equation of motion for the last equality. Noting $e^\chi = \mathcal{C}G(\tau)$, one finds $G'' = -G$. This is precisely the equation satisfied by the vacuum black hole solution, $G = \cos \tau$, demonstrating the consistency between the Schwarzian boundary dynamics and the bulk dilaton solution.

Let us analyze this vacuum solution with $\dot{\tau} = \cos \tau$. Solving this equation gives

$$\dot{\tau} = \cos \tau = 1/\cosh t, \quad (2.17)$$

where we have chosen the integration constant such that $\tau(0) = 0$. As t goes to infinity, the velocity $\dot{\tau} \rightarrow 0$ and $\tau \rightarrow \pi/2$. With $\mathcal{C}\dot{\tau} = e^\chi$, $\ell_{ren} = -2\chi \sim 2t - 2\log 2 \rightarrow \infty$. Hence, the wormhole length and the corresponding complexity grows indefinitely. This indefinite growth is closely tied to the appearance of a singularity in the geometry, since τ is bounded by $\pi/2$ along the boundary trajectory as time t goes to infinity.

The crucial feature of this solution is that the boundary time evolution terminates at the limiting value $\tau = \pi/2$. Although this limit is reached only asymptotically in t , the global coordinate τ itself is bounded. The boundary trajectory therefore accumulates at a finite value of global time τ while the renormalized geodesic length diverges. In the bulk picture, the future left/right horizons are located at $\tau = \mp\mu$. The horizons intersect the boundary precisely at $\tau = \pi/2$. Consequently, as $t \rightarrow \infty$, the boundary trajectory approaches the endpoint of the future horizon. Because the evolution in τ cannot extend beyond $\pi/2$, the bulk spacetime develops a causal pathology behind the horizon. This manifests as the familiar black-hole singularity in the interior region. This well-known bulk black hole geometry is depicted in Figure 1.

We now briefly review the connection between the boundary description of JT gravity discussed above and the SSS duality [4]. The SSS duality can be viewed as providing a nonperturbative completion of JT gravity in terms of an appropriate random matrix model.

When the leading JT bulk dynamics is governed by the Schwarzian Hamiltonian in (2.15), the corresponding eigenstates are scattering states described by modified Bessel functions, and the spectrum is continuous. This reflects the absence of a discrete density of states in the Lorentzian Schwarzian description. According to the SSS duality, however, this apparent continuum should be understood as emerging from an underlying discrete spectrum with typical level spacing of order e^{-S_0} . In the Euclidean framework, the JT disk density of states, $\rho_{JT}(E) = \frac{e^{S_0}}{4\pi^2} \sinh(2\pi\sqrt{E})$ was derived in [4, 14] and subsequently used as input for computing higher-genus corrections in the double-scaling limit of the associated random matrix model. Nevertheless, within the Liouville potential alone, genuine spectral discreteness cannot be realized, as noted above. This apparent clash motivates the introduction of an additional left confining potential, as proposed in [15], which restores discreteness while incorporating the random nature of the spectrum. In the following section, we review this left confining potential and discuss its immediate dynamical consequences.

3 Confining potential and perturbative framework

In this section, we review the left confining potential and formulate a modified version of JT gravity that incorporates this additional potential.

On the matrix model side (see for review [32–34]), we consider an $N \times N$ Hermitian matrix M with eigenvalues λ_i ($i = 1, 2, \dots, N$). Defining $\widehat{Z} = \text{tr} e^{-\beta M} = \sum_i e^{-\beta\lambda_i}$, the averaged matrix-model partition function is obtained by averaging over the eigenvalue

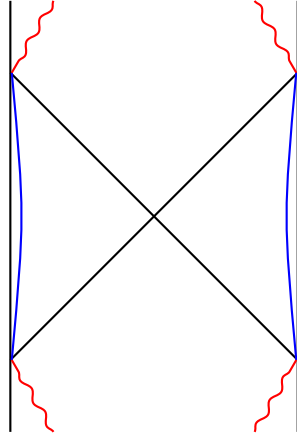


Figure 1: Penrose diagram of bulk AdS₂ spacetime with horizons and boundary cutoff trajectories.

ensemble,

$$\langle \widehat{Z} \rangle_{\vec{\lambda}} \equiv \int d\vec{\lambda} \mathcal{P}(\vec{\lambda}) \widehat{Z}(\vec{\lambda}), \quad (3.1)$$

where $\mathcal{P}(\vec{\lambda})$ is the appropriately normalized JT ensemble weight satisfying $\int d\vec{\lambda} \mathcal{P}(\vec{\lambda}) = 1$. Throughout this work, we take the double-scaling limit in which $N \rightarrow \infty$ while the level-spacing parameter e^{-S_0} is held fixed and small. In the limit, the averaged matrix-model partition function admits the genus expansion as¹

$$\langle \widehat{Z} \rangle_{\vec{\lambda}} \cong e^{S_0} Z_{0,1} + \sum_{g=1}^{\infty} e^{-(2g-1)S_0} Z_{g,1}, \quad (3.3)$$

where \cong indicates equality up to nonperturbative contributions, which are not yet fully understood [16]. The leading semiclassical contribution $e^{S_0} Z_{0,1}$ can be computed from the JT disk density of states ρ_{JT} via a simple Laplace transform, and all remaining higher-order terms can be determined by the so-called topological recursion relations [35–38]. Under the SSS duality [4], the matrix-model expansion described above is mapped term by term to the JT gravity path integral. In this correspondence, $Z_{0,1}$ reproduces the disk amplitude, while $Z_{g,1}$ captures the contributions from genus- g geometries, which we do not review further here.

¹This can be generalized to the connected correlation function of $\widehat{Z}(\beta_1), \widehat{Z}(\beta_2), \dots, \widehat{Z}(\beta_n)$, which has the expansion

$$\langle \widehat{Z}(\beta_1) \widehat{Z}(\beta_2) \cdots \widehat{Z}(\beta_n) \rangle_{\vec{\lambda}, \text{conn}} \cong \sum_{g=0}^{\infty} e^{-(2g-2+n)S_0} Z_{g,n}(\beta_1, \beta_2, \dots, \beta_n). \quad (3.2)$$



Figure 2: A schematic form of the potential $V(q) = e^q + W(q)$, where the left confining potential $W(q)$ becomes $O(1)$ only when q becomes of $-O(e^{S_0})$. With the left confining potential, the spectrum becomes discrete.

As discussed in [15], the Schwarzian Hamiltonian in (2.15) gives rise to a continuous spectrum because the Liouville potential e^q is not confining as $q \rightarrow -\infty$. (Throughout this section and the Appendix, we set $2\mathcal{C} = 1$ for notational simplicity.) To obtain a discrete spectrum, we supplement the system with an additional left confining potential

$$W(X) = W_0(X) + \sum_{n=1}^{\infty} v_n(X) W_n(X) e^{-nS_0}, \quad X = -q e^{-S_0} \quad (3.4)$$

(see Figure 2). Here $W_0(X)$ denotes the leading-order confining potential. It becomes effective only in the regime $q \sim -O(e^{S_0})$, *i.e.* exponentially far to the left in the original Schwarzian coordinate. The functions $v_n(X)$ represent random potentials, introduced in order to reproduce the random nature of the level spacing. With this additional left confining potential, the spectrum becomes discrete once e^{-S_0} is kept finite. The corresponding Hamiltonian takes the form

$$H = e^{-2S_0} p_X^2 + e^{-X e^{S_0}} + W(X), \quad (3.5)$$

with $p_X = -i\partial_X$. We now define a change of variables from the matrix eigenvalues $\vec{\lambda}$ to the collective variables $\{X, \vec{v}(X)\}$ such that

$$\langle \widehat{Z}(\beta_1) \cdots \widehat{Z}(\beta_n) \rangle_{\vec{\lambda}} = \langle Z_H(\beta_1) \cdots Z_H(\beta_n) \rangle_{\vec{v}} \equiv \int \mathcal{D}\vec{v} e^{-\mathcal{U}(\vec{v})} Z_H(\beta_1) \cdots Z_H(\beta_n) \quad (3.6)$$

where $Z_H(\beta) = \text{tr} e^{-\beta H}$ is the quantum-mechanical partition function associated with the Hamiltonian H .

The statistical properties of the random potentials are encoded in the weight functional. At the level of two-point correlations, we take $\mathcal{U}_2 = \frac{1}{2} \sum_n \int dX dY v_n(X) C^{-1}(X - Y) v_n(Y)$, which implements correlations,

$$\langle v_m(X) v_n(Y) \rangle_{\vec{v}} = \delta_{mn} C(X - Y), \quad (3.7)$$

with $\langle v_m(X) \rangle_{\vec{v}} = 0$. We require the correlation function $C(X - Y)$ to be translation invariant. In general, specifying only the two-point function is not sufficient: additional input is required to determine higher-point correlation functions of the random potentials. These higher cumulants encode further statistical data of the ensemble and must be provided in order to fully define the theory beyond leading Gaussian order.

With $\hbar \equiv e^{-S_0}$, the term $e^{-X/\hbar}$ is intrinsically nonperturbative in \hbar . As demonstrated in the Appendix, this term generates an infinitely steep potential barrier in the limit $\hbar \rightarrow 0$, effectively excluding the region $X < 0$ from the physical configuration space. In other words, its only role is to enforce a boundary condition at $X = 0$. Importantly, for $X > 0$ the dynamics are unaffected at any finite order in the perturbative expansion in \hbar . Consequently, when focusing exclusively on the perturbative expansion in powers of \hbar , it is consistent to neglect this nonperturbative contribution and restrict the configuration space to the half-line $X \in [0, \infty)$.

The function $C(X - Y)$ can be reconstructed from the connected two-boundary partition function $Z_{0,2}(\beta_1, \beta_2)$; the details of this derivation are provided in the Appendix. The resulting expressions are

$$C(X) = \delta(X), \quad W_1(X) = \sqrt{2W'_0(X)}, \quad (3.8)$$

where we fix the normalization of $C(X)$ to be unity. Proceeding to the next order, the connected three-boundary amplitude $Z_{0,3}(\beta_1, \beta_2, \beta_3)$, determines the three-point correlation function of the random potential. One finds

$$\langle v_1(X)v_1(Y)v_1(Z) \rangle_{\vec{v}} = -e^{-S_0} Q_\epsilon(X)Q_\epsilon(Y)Q_\epsilon(Z) \quad (3.9)$$

where

$$Q_\epsilon(X) = \epsilon W_1(X)W_0^{\epsilon-1}(X) = W_1(X)\frac{dW_0^\epsilon}{dW_0}. \quad (3.10)$$

Here ϵ is the regularization parameter and the limit $\epsilon \rightarrow 0$ should be taken at the end of the computation. The detailed derivation is again presented in the Appendix. In principle, all higher-point correlation functions of the random potentials must be determined in a similar way. This illustrates that the change of variables from the matrix-model data to the ensemble-averaged quantum-mechanical description is highly nontrivial: the disorder distribution is fixed order by order by matching multi-boundary amplitudes. Finally, the functions W_n are uniquely determined by requiring that the perturbative genus expansion in (3.3) on the matrix-model side be exactly reproduced by the ensemble-averaged quantum mechanics defined above. The matching provides a stringent consistency condition and ensures the equivalence between the two descriptions at the perturbative level.

The leading-order contribution Z_0 is obtained from the limit

$$Z_{0,1}(\beta) = \lim_{\hbar \rightarrow 0} \hbar \operatorname{tr} e^{-\beta(\hbar^2 p_X^2 + e^{-X/\hbar} + W_0(X))}. \quad (3.11)$$

As shown in [15], this expression is solved by

$$2\pi X = \sqrt{W_0(X)} I_1\left(2\pi\sqrt{W_0(X)}\right), \quad (3.12)$$

which follows from an Abel integral equation for $X \geq 0$. (One may further impose $W_n = 0$ for $X < 0$ at least perturbatively.) Thus $W_0(X)$ is determined uniquely. In the Appendix, we further demonstrate that $Z_{1,1}(\beta)$ is correctly reproduced within this framework, up to the expected renormalization effects. This agreement is far from trivial: the required input data, namely the correlation function $C(X)$ and the function W_1 are already fixed independently. This matching therefore provides a nontrivial and additional consistency check of the framework. Further checks of higher-order contributions $Z_{g,n}$ as well as of the associated topological recursion relations, are required for a full validation of the construction. We leave these investigations for future work.

To compute physical quantities of interest, such as the complexity, we use the so-called quenched version,

$$\langle O \rangle_q = \left\langle \frac{\operatorname{tr} O e^{-\beta H}}{\operatorname{tr} e^{-\beta H}} \right\rangle_{\vec{v}}, \quad (3.13)$$

where the quantum-mechanical trace is performed first and the ensemble average is taken afterward. In this quenched average, the random potential in a given realization is fixed in time during the quantum-mechanical evolution. This, for instance, leads to plateau behavior in the presence of the random potential for a given sample. After performing the ensemble average, the plateau behavior remains while fluctuations are averaged out. This quenched version is the one we consider in this work for any physical observables. In [15], we checked numerically, for a given random-potential sample, that the geodesic length—identified with the Krylov complexity—exhibits the anticipated behavior: a ramp, a top, a slope, and finally a plateau² (see Figure 3).

In the so-called annealed average, one performs the ensemble average first and then takes the quantum-mechanical trace,

$$\langle O \rangle_a = \frac{\operatorname{tr} O \langle e^{-\beta H} \rangle_{\vec{v}}}{\operatorname{tr} \langle e^{-\beta H} \rangle_{\vec{v}}}. \quad (3.14)$$

Due to the averaging over the potential first, the random potential is no longer fixed in time in the path-integral formulation. Since the realization of the random potential can

²Some related works include [39–50].

change over time, the spectrum becomes effectively continuous and full phase cancellation between different states never occurs. Consequently, in this annealed case, the complexity grows linearly in time indefinitely and never reaches a plateau. In this work, we do not use the annealed average for any physical observables.

For the free energy of the system, one is required to compute

$$\langle \ln Z_H \rangle_{\bar{v}} = \lim_{n \rightarrow 0} (\langle Z_H^n \rangle_{\bar{v}} - 1) / n, \quad (3.15)$$

which corresponds to the quenched prescription. The expression on the right-hand side can be evaluated using the replica trick, as is well known in disordered systems. We emphasize that

$$\langle \ln Z_H \rangle_{\bar{v}} \neq \ln \langle Z_H \rangle_{\bar{v}}, \quad (3.16)$$

and therefore care must be taken in this respect.

4 Resolution of black hole singularities

If we introduce the extra confining potential W , the boundary dynamics is significantly modified once this potential becomes relevant, which occurs at time scales $t \sim O(e^{S_0})$ or equivalently $\chi \sim -O(e^{S_0})$. The total potential takes the form

$$V(\chi) = \frac{e^{2\chi}}{2\mathcal{C}} + W. \quad (4.1)$$

Accordingly, the equation of motion in (2.16) becomes

$$\mathcal{C}\ddot{\chi} = \mathcal{C}G''\dot{\tau} = \mathcal{C}GG'' = -\frac{e^{2\chi}}{\mathcal{C}} - \partial_\chi W. \quad (4.2)$$

The physical picture is transparent. At early times, the effect of the confining potential W is negligible, and the evolution is governed primarily by the Liouville term. As $-\chi$ increases, the velocity $\dot{\chi}$ approaches an approximately constant value and remains nearly constant until $\chi \sim -O(e^{S_0})$. This regime corresponds to the well-known linear growth of complexity. Once χ reaches this exponentially large negative value, however, the confining potential becomes important and qualitatively alters the subsequent evolution.

As time evolves further, the system eventually reaches the left turning point $\chi_{ltp} \sim -O(e^{S_0})$, at which the velocity vanishes, $\dot{\chi} = G'$. At this point, $\dot{\tau} = G = e^\chi/\mathcal{C}$ attains its minimum value. Therefore,

$$\dot{\tau} \geq \frac{e^{\chi_{ltp}}}{\mathcal{C}}. \quad (4.3)$$

Since $\dot{\tau}$ remains strictly positive, $\tau(t)$ continues to increase monotonically and grows indefinitely beyond $\tau = \pi/2$. From the viewpoint of the cutoff trajectory, this behavior

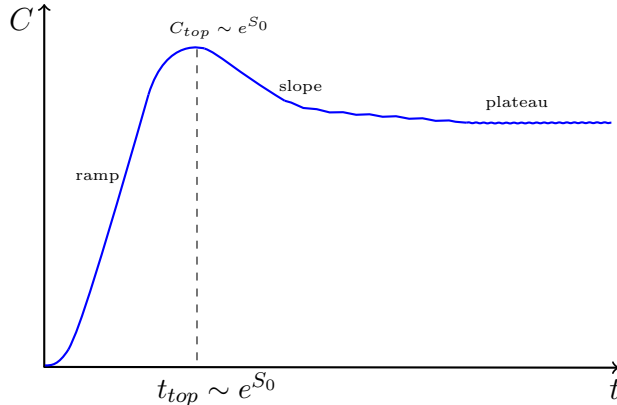


Figure 3: Schematic diagram for complexity vs time. The typical behavior of ramp, top, slope and plateau of the complexity or equivalently the geodesic length is depicted.

corresponds to an effective resolution of the would-be singularity. At the turning point, the spread complexity reaches its maximal value, followed by the slope region. As we argue below, beyond this point the classical description of the boundary evolution gradually ceases to be valid: when the spread complexity of the quantum state becomes of order e^{S_0} , quantum effects become significant and the classical approximation begins to break down.

In particular, once the random potential is included, the spectrum exhibits random-matrix statistics: the level spacing is of order e^{-S_0} and displays level repulsion. Accordingly, at time scales $t \sim O(e^{S_0})$, the evolution begins to deviate from purely classical motion. Nevertheless, the Ehrenfest theorem continues to hold. We now consider the Hamiltonian

$$H = \frac{p_q^2}{2\mathcal{C}} + V(q), \quad V(q) = W + \frac{e^q}{2\mathcal{C}}, \quad (4.4)$$

with eigenvalues E_n and eigenstates $|n\rangle$. The thermofield double (TFD) state evolved by $H_{\text{tot}} = 2H$ is

$$|\psi(t)\rangle_{\text{tfd}} = \frac{1}{\sqrt{Z}} \sum_n e^{-(\frac{\beta}{2} + 2it)E_n} |n, n\rangle. \quad (4.5)$$

where $|n, m\rangle \equiv |n\rangle_l \otimes |m\rangle_r$.

The expectation values satisfy

$$\begin{aligned} \frac{d}{dt} \langle q \rangle_{\text{tfd}} &= -i \langle [q, 2H] \rangle_{\text{tfd}} = \frac{2}{\mathcal{C}} \langle p_q \rangle_{\text{tfd}}, \\ \frac{d}{dt} \langle p_q \rangle_{\text{tfd}} &= -i \langle [p_q, 2H] \rangle_{\text{tfd}} = -2 \langle \partial_p V \rangle_{\text{tfd}}, \end{aligned} \quad (4.6)$$

which together imply the quantum analogue of the classical equation of motion,

$$\mathcal{C} \frac{d^2}{dt^2} \langle \chi \rangle_{tfd} = -\langle \partial_\chi V \rangle_{tfd}. \quad (4.7)$$

More explicitly,

$$\frac{d}{dt} \langle q \rangle_{tfd} = \frac{2i}{Z} \sum_{m,n} e^{-\frac{\beta}{2}(E_m+E_n)} e^{2it(E_m-E_n)} (E_m - E_n) \langle m, m | q | n, n \rangle. \quad (4.8)$$

For $t \gg e^{S_0}$, the rapidly oscillating phases $e^{2it(E_m-E_n)}$ undergo erratic cancellations due to the random-matrix nature of the spectrum. As a result, the off-diagonal contributions ($m \neq n$) average to zero, yielding

$$\frac{d}{dt} \langle q \rangle_{tfd} \sim 0, \quad (4.9)$$

which characterizes the plateau regime [5, 34, 39]. This is also consistent with the fact $\langle q \rangle_{tfd}$ becomes time independent in the plateau regime ignoring those erratic phase canceling contributions; this can be explicitly shown as

$$\langle q \rangle_{tfd} = \frac{1}{Z} \sum_{m,n} e^{-\frac{\beta}{2}(E_m+E_n)} e^{2it(E_m-E_n)} \langle m, m | q | n, n \rangle \sim \frac{1}{Z} \sum_n e^{-\beta E_n} \langle n, n | q | n, n \rangle, \quad (4.10)$$

where the last relation follows by considering the phase cancellation of the middle expression for $m \neq n$. In this regime, one may also show that $-i\langle [p_q, 2H] \rangle_{tfd} = -2\langle \partial_q V \rangle_{tfd} \sim 0$ by a similar argument. Thus, the behavior of the complexity near the plateau region admits a natural quantum-mechanical explanation: at late times, phase decoherence induced by random-matrix level statistics suppresses coherent evolution, leading to an effective freezing of the expectation values.

Applying the above result to the boundary dynamics, we find that the evolution begins to deviate from purely classical behavior once the system passes the top region. In particular, the vacuum expectation value of the renormalized geodesic length, $\langle \ell_{ren} \rangle_{tfd} = -2\langle \chi \rangle_{tfd}$ starts to decrease and eventually approaches a constant plateau value. In this late-time regime, the boundary trajectory remains nearly parallel to spatial infinity. Although small, irregular fluctuations persist due to the underlying random-matrix dynamics, the overall motion is effectively frozen at the level of expectation values. This qualitative behavior is illustrated in Figure 3. Furthermore, since $\langle \dot{\tau} \rangle_{tfd} = \langle e^\chi \rangle_{tfd} / \mathcal{C} \sim \text{const.}$, it follows that $\tau(t)$ continues to grow linearly with t even in the plateau regime. Consequently, the boundary global time $\tau(t)$ never stalls, and the would-be singularity is completely avoided. The resolution of the singularity is therefore dynamical in nature and is ultimately governed by the behavior of the spread complexity³.

³In a recent paper [51], the spread complexity is also used to compute the Hilbert space dimension.

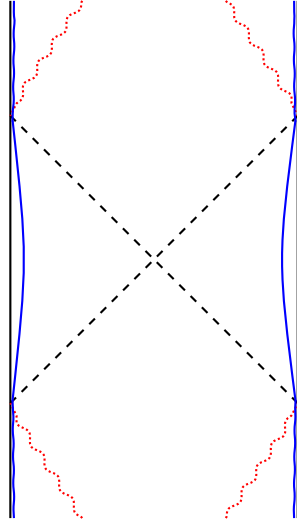


Figure 4: The boundary cutoff trajectories, depicted by blue lines, do not touch the AdS boundaries depicted by black lines, and extend to the upper and lower sides forever. The dashed diagonal lines denote the would-be horizons and the dotted red lines do the would-be singularities.

5 Bulk view of the resolution

In this section, we explore the bulk implications of the singularity resolution. We begin by discussing the disappearance of the future horizons and the resulting apparent causal connection between the left and right boundaries. We then analyze the corresponding modifications of the bulk dilaton profile. (See [52] for some related issues.)

As the boundary time coordinates $\tau_{r/l}(t)$ grow indefinitely, the bulk spacetime extends across the entire strip. As illustrated in Figure 4, the left and right future horizons disappear completely. In contrast to the original eternal black-hole geometry—where the two boundary trajectories are entirely causally disconnected—the modified geometry allows causal contact between the left and right boundaries. Given this causal connection, it is natural to ask whether it is possible to send a physical signal from one side to the other.

From the view point of the dual TFD state [53], it is clear that one cannot send a physical signal from one side to the other since the left and right systems are noninteracting with each other. To show this explicitly, let us perturb the Hamiltonian of the right-boundary system by

$$\delta H_r = J_r(t) \mathcal{O}_r(t) \tag{5.1}$$

where $\mathcal{O}_r = 1 \otimes \mathcal{O}$ acting on the right hand side only. We try to detect this change from

the left side by considering the expectation value of some operator

$$\mathcal{X}_l = \mathcal{X} \otimes 1 \tag{5.2}$$

Its induced change is given by

$$\delta \langle \mathcal{X}_l(t) \rangle_{tfd} = i \int_{-\infty}^t dt' \langle [\delta H(t'), \mathcal{X}_l(t)] \rangle_{tfd} = 0, \tag{5.3}$$

which vanishes identically since $[\mathcal{O}_r(t'), \mathcal{X}_l(t)] = 0$. Hence from the left side, the change in the right side cannot be detected.

From the bulk perspective, once the horizons disappear the geometry appears transparent, suggesting that a signal emitted from one side may propagate to the other without obstruction. However, a more careful analysis reveals an important limitation. A signal sent from the right boundary at a time $t_s \sim O(1)$ reaches the left boundary only at a parametrically late time $t_a = \kappa(t_s)e^{S_0}$ where $\kappa(t_s) \sim O(1)$. In principle, this arrival time can be determined from the boundary dynamics. It also obeys the inequality $\kappa(t_s) \geq \kappa(t_h)$ where is defined by $\tau(t_h) = \pi/2$. At this exponentially large time scale, the spread complexity of the TFD state has already approached its plateau value. The system is then in a regime of extreme complexity and effective randomness. In such a state, any small perturbation becomes indistinguishable from the intrinsic background fluctuations. Moreover, by the time it reaches the opposite boundary, the signal itself has been thoroughly scrambled and fully delocalized over the available Hilbert space. Therefore, despite the apparent geometric transparency, no practically recoverable information can be transmitted in this manner.

The situation here is reminiscent of the island scenario [54–56], where complexity likewise plays a crucial role. In the semiclassical description, the island degrees of freedom appear to reside behind the horizon. However, in the full quantum description they are encoded in the radiation degrees of freedom. This apparent tension with causality in the semiclassical picture is resolved, once computational complexity is taken into account. Although the information is, in principle, present in the radiation, extracting it requires decoding operations of order $\mathcal{O}(e^S)$ complexity. Such operations are exponentially difficult in the entropy and therefore effectively inaccessible in practice. In this way, complexity restores operational causality: while the information is not fundamentally lost, it cannot be retrieved by any feasible physical process.

We now turn to the corresponding bulk description of the dilaton field, incorporating the modification of the boundary dynamics. Note that, in the presence of the energy–momentum tensor T_{ab} , the dilaton satisfies

$$\nabla_a \nabla_b \phi - g_{ab} \nabla^2 \phi + g_{ab} \phi = -T_{ab}. \tag{5.4}$$

Assuming that the extra matter sector introduced above is independent of the dilaton field, the bulk spacetime remains AdS_2 , with the metric taken in its global form as given in (2.5). Motivated by the form in (2.9), we assume that the dilaton takes the form

$$\phi = \mathcal{C} \left(\frac{G(\tau)}{\cos \mu} - \cos \mu K(\tau) \right), \quad (5.5)$$

where $G(\tau)$ is given by the solution of (4.2), whose explicit form can, in principle, be obtained once W is specified. Using the above dilaton equation, one finds

$$\begin{aligned} T_{\tau\tau}/\mathcal{C} &= -2K \cos \mu, \\ T_{\tau\mu}/\mathcal{C} &= -2K' \sin \mu, \\ T_{\mu\mu}/\mathcal{C} &= -\frac{G + G'' - 2K}{\cos \mu} - (K - K'') \cos \mu. \end{aligned} \quad (5.6)$$

Since we do not want the energy-momentum tensor to have a singular contribution along the cutoff trajectories, the $1/\cos \mu$ term in $T_{\mu\mu}$ must be absent. This requirement leads to the condition

$$K(\tau) = \frac{1}{2}(G + G'') = -\frac{1}{2}e^{-\chi}\partial_\chi W \quad (5.7)$$

where χ is related to τ by the relation $e^\chi = \mathcal{C}G(\tau)$. Hence, the dilaton and the bulk energy-momentum tensor are uniquely determined once the left confining potential is specified.

A few comments are in order. First, in JT theory without modification, the bulk force is attractive, and any mass inevitably falls into the horizon. As noted in [9], this attractive nature is related to the linear growth of the spread complexity in the ramp region. Without our modification, the linear growth continues, as we have already mentioned. The relevant force in this case is given by

$$F_- = -\frac{\langle e^{2\chi} \rangle}{\mathcal{C}}, \quad (5.8)$$

which is negative definite. The turnaround is controlled by a new force,

$$F_+ = -\langle \partial_\chi W \rangle, \quad (5.9)$$

which is positive definite (in an averaged sense over the random contributions). Hence, in this regime, around the top, the dilaton becomes negative in the bulk, while remaining positive at the boundary.

In the plateau region, the expectation values of any operator become constant, using the same argument as in (4.10). Hence, in this region,

$$\phi = \mathcal{C} \left(\frac{a}{\cos \mu} - \cos \mu b \right), \quad (5.10)$$

where $a = \langle G \rangle_{plateau}$ and $b = \langle K \rangle_{plateau}$. Therefore, in the plateau regime, the dilaton becomes stationary in the τ coordinate. A precise estimation of a and b as functions of time t would be of interest, but we leave this for future work.

Next, we turn to the discussion of the bulk energy. This can be constructed from T_{ab} using covariant conservation:

$$\nabla_a(T^a_b f^b) = 0, \quad (5.11)$$

where $f = \partial_\tau$ is the Killing vector satisfying the Killing equation $\nabla_a f_b + \nabla_b f_a = 0$. This implies the ordinary conservation law

$$\partial_a(\sqrt{-g}T^a_\tau) = 0, \quad (5.12)$$

from which one can define the bulk energy as

$$E_{bulk} = - \int_{-\pi/2}^{\pi/2} d\mu \sqrt{-g} \langle T^r_\tau \rangle = -4\mathcal{C} \langle K \rangle, \quad (5.13)$$

which is negative definite. Hence, the bulk energy induced by the left confining potential is negative. This negative-energy contribution becomes relevant at times $t \sim O(e^{S_0})$ deriving the singularity resolution and the turnaround.

Finally, using the energy-momentum tensor, one may verify that

$$-\mathcal{C} \frac{d}{dt} \text{Sch} \left(\tan \frac{\tau(t)}{2}, t \right) = (\dot{\tau})^2 T_{\tau\mu} \quad (5.14)$$

holds along the cut-off boundary. This relation may be interpreted as the bulk force, induced by the modification of the energy-momentum tensor, acting on the boundary trajectories. It therefore leads to a corresponding modification of the boundary dynamics.

6 Conclusions

In this work, we have demonstrated that introducing a left confining potential in JT gravity provides a natural and dynamical mechanism for resolving black hole singularities. Requiring a discrete bulk spectrum with random statistics naturally leads to the existence of a left confining potential which becomes relevant only when the renormalized geodesic length is of order e^{S_0} . In the absence of this potential, the boundary cutoff trajectory asymptotes to the AdS boundaries, corresponding to an ever-growing wormhole length and the formation of a bulk singularity. With the confining term included, however, the evolution develops a turning point at $\chi \sim -O(e^{S_0})$, where the effective repulsive force prevents the indefinite growth of the wormhole length. Then, the boundary trajectory continues to evolve beyond the would-be endpoint, eliminating the geometric pathology.

The singularity resolution is therefore not imposed by hand but emerges dynamically from the discreteness of the spectrum. The Krylov spread complexity, which is identified with the wormhole length, then settles into a plateau after reaching a maximum, rather than growing indefinitely.

From the bulk perspective, this modification drastically alters the causal structure of spacetime. The would-be future horizons disappear and the left and right boundaries become causally connected. However, we argued that, in practice, no information can be transferred between them. Any signal sent from one boundary reaches the other only at time scales $t \sim O(e^{S_0})$, a regime where the system becomes extremely complicated and effectively random. At this stage, the signal is thoroughly scrambled over the Hilbert space, making it indistinguishable from the background. Thus, the semiclassical paradox of causality violation is resolved by the extreme complexity of the quantum state. The “complexity barrier” then emerges as the quantum successor to the classical event horizon.

Our results suggest that the resolution of the singularity is an inherently non-classical phenomenon, arising directly from the discrete and random nature of the underlying spectrum. The smooth geometric description breaks down at time scale of $O(e^{S_0})$ in the plateau regime, where the physics is inaccessible in semiclassical analyses and is governed by the random statistics of the energy levels.

Several important questions remain for future study. A full verification of the framework requires matching higher-order contributions $Z_{g,n}$ and establishing compatibility with topological recursion beyond the leading orders. The bulk energy associated with the left confining potential turns out to be negative, and becomes relevant at times $t \sim O(e^{S_0})$. It would also be interesting to clarify the precise bulk interpretation of the random potential. While this study focused on two-dimensional gravity, it would be of great interest to investigate whether similar mechanisms can be generalized to higher-dimensions.

Acknowledgement

DB was supported in part by Basic Science Research Program through NRF funded by the Ministry of Education (2018R1A6A1A06024977). C.K. was supported by NRF Grant 2022R1F1A1074051. S.-H.Y. was supported in part by NRF grant funded by the Korea government(MSIT) RS-2025-00553127.

Appendix

A Perturbative expansions of the partition function

We consider a one-dimensional quantum system with Hamiltonian $H = p^2 + V(X)$ and aim to compute the canonical partition function

$$Z_H = \int dX \langle X | e^{-\beta H} | X \rangle \quad (\text{A.1})$$

as an expansion in powers of \hbar . To this end, we introduce the Wigner transform of an operator \hat{O} ,

$$O_W(X, p) := \int_{-\infty}^{\infty} dy e^{-\frac{i}{\hbar}py} \left\langle X + \frac{y}{2} \left| \hat{O} \right| X - \frac{y}{2} \right\rangle. \quad (\text{A.2})$$

For $\hat{O} = e^{-\beta H}$, the partition function can be written in phase-space form as

$$Z_H = \frac{1}{2\pi\hbar} \int dX dp (e^{-\beta H})_W(X, p). \quad (\text{A.3})$$

It is useful to examine the symmetry properties of the Wigner kernel. Let us define

$$K(\hbar, X) := \int dp dy e^{-\frac{i}{\hbar}py} \left\langle X + \frac{y}{2} \left| e^{-\beta H} \right| X - \frac{y}{2} \right\rangle. \quad (\text{A.4})$$

Under the transformation $p \rightarrow -p$, one finds

$$K(\hbar, X) = \int dp dy e^{+\frac{i}{\hbar}py} \left\langle X + \frac{y}{2} \left| e^{-\beta H} \right| X - \frac{y}{2} \right\rangle = K(-\hbar, X). \quad (\text{A.5})$$

This symmetry implies that $K(\hbar, X)$ admits an expansion containing only even powers of \hbar . Indeed one may show that the partition function takes the standard Wigner–Kirkwood form [57, 58]

$$Z_H = \int \frac{dX dp}{2\pi\hbar} e^{-\beta(p^2 + V(X))} \left[1 + \sum_{g=1}^{\infty} \hbar^{2g} A_{2g}(X) \right], \quad (\text{A.6})$$

where the coefficient functions $A_{2g}(X)$ are local expressions constructed from $V(X)$ and its derivatives. This expansion provides a systematic semiclassical approximation to the quantum partition function. At order \hbar^2 , the coefficient is given by the well-known expression

$$A_2(X) = \frac{1}{12} (\beta^3 (V')^2 - 2\beta^2 V''). \quad (\text{A.7})$$

Performing the Gaussian integral over p , one finally obtains

$$Z_H = \frac{1}{\hbar\sqrt{4\pi\beta}} \int dX e^{-\beta V(X)} \left[1 + \frac{1}{12} (\beta^3 (V')^2 - 2\beta^2 V'') \hbar^2 + O(\hbar^4) \right]. \quad (\text{A.8})$$

Some explicit expressions for A_{2g} can be further found in [59].

For the problem of interest, we identify the semiclassical expansion parameter as $\hbar = e^{-S_0}$ and consider the Hamiltonian $H = p^2 + V(X)$ where the potential has the form $V(X) = W(X) + e^{-X/\hbar}$ and p has the standard form $p = -i\hbar\partial_X$.

The term $e^{-X/\hbar}$ is intrinsically nonperturbative in \hbar . Indeed, it does not admit a Taylor expansion around $\hbar = 0$, since

$$(\partial/\partial\hbar)^n e^{-X/\hbar}|_{\hbar=0} \quad (\text{A.9})$$

is ill-defined for all n . In the semiclassical limit $\hbar \rightarrow 0$, this term generates an infinitely steep potential barrier, effectively forbidding access to the region $X < 0$. As a consequence, the nonperturbative contribution $e^{-X/\hbar}$ enforces a boundary condition at $X = 0$, while leaving the dynamics in the region $X > 0$ unaffected at any finite order in perturbation theory.

If one is interested purely in the perturbative expansion in powers of \hbar , it is therefore consistent to discard such nonperturbative effects and restrict the configuration space to the half-line $X \in [0, \infty)$. In this approximation, the partition function reduces to

$$Z_H \cong \frac{1}{\hbar\sqrt{4\pi\beta}} \int_0^\infty dX e^{-\beta W(X)} \left[1 + \frac{1}{12} (\beta^3 (W')^2 - 2\beta^2 W'') \hbar^2 + O(\hbar^4) \right]. \quad (\text{A.10})$$

More generally, the complete perturbative Wigner-Kirkwood expansion follows directly from (A.6) upon replacing $V(X)$ by $W(X)$ and restricting the integration domain to the half-line $[0, \infty)$. All effects associated with the exponential term $e^{-X/\hbar}$ are nonperturbative in \hbar and are thus consistently omitted within this purely perturbative treatment.

With the perturbative expression for the partition function at hand, we may now perform the ensemble average. The result takes the form

$$\langle Z_H(\beta) \rangle_{\vec{v}} \cong Z_{0,1} \hbar^{-1} + \sum_{g=1}^{\infty} Z_{g,1} \hbar^{2g-1} \quad (\text{A.11})$$

It is manifest that the ensemble average generates only additional even powers of \hbar , so that the final result naturally organizes itself into a genus expansion.

At leading order, one finds

$$Z_{0,1} = \frac{1}{\sqrt{16\pi\beta^3}} e^{\frac{\pi^2}{\beta}} = \frac{1}{\sqrt{4\pi\beta}} \int_0^\infty dX e^{-\beta W_0(X)}. \quad (\text{A.12})$$

This expression can be inverted by an inverse Laplace transform, yielding the potential $W_0(X)$ given in (3.12). A detailed derivation of this inversion was presented in the appendix of Ref. [15].

One may also compute the connected two-boundary partition function $Z_{0,2}(\beta_1, \beta_2)$ directly on the quantum-mechanical side. It is given by

$$Z_{0,2}(\beta_1, \beta_2) = \frac{\sqrt{\beta_1\beta_2}}{4\pi} \int_0^\infty dX W_1(X) \int_0^\infty dY W_1(Y) e^{-\beta_1 W_0(X) - \beta_2 W_0(Y)} C(X - Y). \quad (\text{A.13})$$

With the known form $Z_{0,2} = \frac{\sqrt{\beta_1\beta_2}}{2\pi(\beta_1+\beta_2)}$ [4], and taking double inverse Laplace transforms of $4\pi Z_{0,2}/\sqrt{\beta_1\beta_2}$ to the variables $W_0(X)$ and $W_0(Y)$ of the both sides, one finds

$$2\delta(W_0(X) - W_0(Y)) = \frac{W_1(X) W_1(Y)}{W_0'(X) W_0'(Y)} C(X - Y), \quad (\text{A.14})$$

With the translation invariance of the correlation function $C(X)$, this equation admits a unique solution, given by (3.8), up to an overall normalization. We fix this normalization to unity

At the next order in \hbar in the one-boundary partition function, the coefficient $Z_{1,1}$ is given by

$$Z_{1,1}(\beta) = \frac{\beta^{\frac{3}{2}}}{4\sqrt{\pi}} \int_0^\infty dX e^{-\beta W_0(X)} \left[W_1(X) W_1(X + \alpha\epsilon) \delta_\epsilon(0) + \frac{1}{6} (\beta(W_0')^2 - 2W_0'') \right]. \quad (\text{A.15})$$

Here $\delta_\epsilon(x) = \frac{1}{\epsilon} e^{-\frac{\pi x^2}{\epsilon^2}}$ is a regulated delta function, and $\alpha\epsilon$ denotes the asymmetric point-splitting parameter. We would like to match this expression with the known result [4]

$$Z_{1,1}(\beta) = \frac{\sqrt{\beta}}{12\sqrt{\pi}} (\beta + \pi^2). \quad (\text{A.16})$$

Using the relation $W_1 = \sqrt{2W_0'}$, the right-hand side of (A.15) can be rearranged into

$$\frac{\beta^{3/2}}{4\sqrt{\pi}} \left[2 \frac{\delta_\epsilon(0)}{\beta} + \frac{1}{3} + (\alpha\epsilon\delta_\epsilon(0) - 1/6) \int_0^\infty dX W_0'' e^{-\beta W_0(X)} \right]. \quad (\text{A.17})$$

Reproducing the known answer requires the elimination of the last term in parentheses. This fixes the asymmetric point-splitting parameter through $\alpha\epsilon\delta_\epsilon(0) = 1/6$, which implies $\alpha = 1/6$. Finally, by subtracting an appropriate local counterterm, the divergent quantity $\delta_\epsilon(0)$ may be replaced by its renormalized value $r_1 = \pi^2/6$. With this prescription, the expression above precisely reproduces the known result for $Z_{1,1}(\beta)$.

To determine the three-point function in (3.9), we begin with the connected three-boundary amplitude on the matrix-model side, $Z_{0,3} = \sqrt{\beta_1\beta_2\beta_3}/\pi^{3/2}$. We require that this result be reproduced by the connected three-boundary contribution computed in the ensemble-averaged quantum-mechanical description. This matching condition leads to

$$\begin{aligned} \hbar Z_{0,3} = & -\frac{\sqrt{\beta_1\beta_2\beta_3}}{8\pi^{3/2}} \int_0^\infty dX W_1(X) \int_0^\infty dY W_1(Y) \int_0^\infty dZ W_1(Z) \\ & \times \langle v_1(X) v_1(Y) v_1(Z) \rangle_{\vec{v}} e^{-(\beta_1 W_0(X) + \beta_2 W_0(Y) + \beta_3 W_0(Z))}. \end{aligned} \quad (\text{A.18})$$

Substituting the expression (3.9) for the three-point correlator together with $W_1 = \sqrt{2\overline{W}_0'}$, and taking the limit $\epsilon \rightarrow 0$ at the end of the computation, one verifies that the right-hand side precisely reproduces the matrix-model result.

One may hope that this procedure can be iterated systematically to higher orders. In particular, at each order in \hbar , the known coefficient $Z_{g,1}(\beta)$ should determine the corresponding correction $W_g(X)$ to the effective potential. If this structure persists, the full perturbative expansion of the effective potential could be reconstructed recursively from the genus expansion of the ensemble-averaged partition function. Establishing this recursive relation in a precise manner, however, requires additional consistency checks, which we leave for future investigation.

References

- [1] R. Jackiw, “Lower Dimensional Gravity,” Nucl. Phys. B **252**, 343-356 (1985).
- [2] C. Teitelboim, “Gravitation and Hamiltonian Structure in Two Space-Time Dimensions,” Phys. Lett. B **126**, 41-45 (1983).
- [3] A. Almheiri and J. Polchinski, “Models of AdS₂ backreaction and holography,” JHEP **11**, 014 (2015) [arXiv:1402.6334 [hep-th]].
- [4] P. Saad, S. H. Shenker and D. Stanford, “JT gravity as a matrix integral,” [arXiv:1903.11115 [hep-th]].
- [5] L. Susskind, “Three Lectures on Complexity and Black Holes,” Springer, 2020, ISBN 978-3-030-45108-0, 978-3-030-45109-7 [arXiv:1810.11563 [hep-th]].
- [6] L. Susskind, “Computational Complexity and Black Hole Horizons,” Fortsch. Phys. **64**, 24-43 (2016) [arXiv:1403.5695 [hep-th]].
- [7] L. Susskind, “Entanglement is not enough,” Fortsch. Phys. **64**, 49-71 (2016) [arXiv:1411.0690 [hep-th]].
- [8] A. R. Brown, H. Gharibyan, H. W. Lin, L. Susskind, L. Thorlacius and Y. Zhao, “Complexity of Jackiw-Teitelboim gravity,” Phys. Rev. D **99**, no.4, 046016 (2019) [arXiv:1810.08741 [hep-th]].
- [9] L. Susskind, “Complexity and Newton’s Laws,” Front. in Phys. **8**, 262 (2020) [arXiv:1904.12819 [hep-th]].

- [10] L. Susskind and Y. Zhao, “Complexity and Momentum,” JHEP **03**, 239 (2021) [arXiv:2006.03019 [hep-th]].
- [11] J. Maldacena, D. Stanford and Z. Yang, “Conformal symmetry and its breaking in two dimensional Nearly Anti-de-Sitter space,” PTEP **2016**, no.12, 12C104 (2016) [arXiv:1606.01857 [hep-th]].
- [12] D. Harlow and D. Jafferis, “The Factorization Problem in Jackiw-Teitelboim Gravity,” JHEP **02**, 177 (2020) [arXiv:1804.01081 [hep-th]].
- [13] D. Bagrets, A. Altland and A. Kamenev, “Sachdev–Ye–Kitaev model as Liouville quantum mechanics,” Nucl. Phys. B **911**, 191-205 (2016) [arXiv:1607.00694 [cond-mat.str-el]].
- [14] D. Stanford and E. Witten, “Fermionic Localization of the Schwarzian Theory,” JHEP **10**, 008 (2017) [arXiv:1703.04612 [hep-th]].
- [15] D. Bak, C. Kim and S. H. Yi, “Discrete bulk spectrum in Jackiw-Teitelboim theory,” Phys. Rev. D **112** (2025) no.12, 126002 [arXiv:2503.00346 [hep-th]].
- [16] T. G. Mertens and G. J. Turiaci, “Solvable models of quantum black holes: a review on Jackiw–Teitelboim gravity,” Living Rev. Rel. **26**, no.1, 4 (2023) [arXiv:2210.10846 [hep-th]].
- [17] G. J. Turiaci, “Les Houches lectures on two-dimensional gravity and holography,” [arXiv:2412.09537 [hep-th]].
- [18] V. Balasubramanian, M. Decross, A. Kar and O. Parrikar, “Quantum Complexity of Time Evolution with Chaotic Hamiltonians,” JHEP **01**, 134 (2020) [arXiv:1905.05765 [hep-th]].
- [19] V. Balasubramanian, P. Caputa, J. M. Magan and Q. Wu, “Quantum chaos and the complexity of spread of states,” Phys. Rev. D **106**, no.4, 046007 (2022) [arXiv:2202.06957 [hep-th]].
- [20] V. Balasubramanian, J. M. Magan and Q. Wu, “Tridiagonalizing random matrices,” Phys. Rev. D **107**, no.12, 126001 (2023) [arXiv:2208.08452 [hep-th]].
- [21] J. Erdmenger, S. K. Jian and Z. Y. Xian, “Universal chaotic dynamics from Krylov space,” JHEP **08**, 176 (2023) [arXiv:2303.12151 [hep-th]].

- [22] E. Rabinovici, A. Sánchez-Garrido, R. Shir and J. Sonner, “A bulk manifestation of Krylov complexity,” *JHEP* **08**, 213 (2023) [arXiv:2305.04355 [hep-th]].
- [23] V. Balasubramanian, J. M. Magan, P. Nandi and Q. Wu, “Spread complexity and the saturation of wormhole size,” *Phys. Rev. D* **113**, no.4, 046004 (2026) [arXiv:2412.02038 [hep-th]].
- [24] P. Nandy, A. S. Matsoukas-Roubeas, P. Martínez-Azcona, A. Dymarsky and A. del Campo, “Quantum dynamics in Krylov space: Methods and applications,” *Phys. Rept.* **1125-1128** (2025), 1-82 [arXiv:2405.09628 [quant-ph]].
- [25] S. Baiguera, V. Balasubramanian, P. Caputa, S. Chapman, J. Haferkamp, M. P. Heller and N. Y. Halpern, “Quantum complexity in gravity, quantum field theory, and quantum information science,” *Phys. Rept.* **1159**, 1-77 (2026) [arXiv:2503.10753 [hep-th]].
- [26] E. Rabinovici, A. Sánchez-Garrido, R. Shir and J. Sonner, “Krylov Complexity,” [arXiv:2507.06286 [hep-th]].
- [27] K. Jensen, “Chaos in AdS₂ Holography,” *Phys. Rev. Lett.* **117**, no.11, 111601 (2016) [arXiv:1605.06098 [hep-th]].
- [28] J. Engelsöy, T. G. Mertens and H. Verlinde, “An investigation of AdS₂ backreaction and holography,” *JHEP* **07**, 139 (2016) [arXiv:1606.03438 [hep-th]].
- [29] T. G. Mertens, G. J. Turiaci and H. L. Verlinde, “Solving the Schwarzian via the Conformal Bootstrap,” *JHEP* **08**, 136 (2017) [arXiv:1705.08408 [hep-th]].
- [30] A. Kitaev and S. J. Suh, “The soft mode in the Sachdev-Ye-Kitaev model and its gravity dual,” *JHEP* **05**, 183 (2018) [arXiv:1711.08467 [hep-th]].
- [31] D. Bak, C. Kim and S. H. Yi, “Quantization of Jackiw-Teitelboim gravity with a massless scalar,” *JHEP* **05**, 045 (2023) [arXiv:2303.05057 [hep-th]].
- [32] M. L. Mehta, *Random matrices*, third ed., Pure and Applied Mathematics, vol. 142, Elsevier/Academic Press, Amsterdam, 2004.
- [33] B. Eynard, T. Kimura and S. Ribault, “Random matrices,” [arXiv:1510.04430 [math-ph]].
- [34] J. S. Cotler, G. Gur-Ari, M. Hanada, J. Polchinski, P. Saad, S. H. Shenker, D. Stanford, A. Streicher and M. Tezuka, “Black Holes and Random Matrices,” *JHEP* **05**, 118 (2017) [erratum: *JHEP* **09**, 002 (2018)] [arXiv:1611.04650 [hep-th]].

- [35] B. Eynard, “Topological expansion for the 1-Hermitian matrix model correlation functions,” *JHEP* **11**, 031 (2004) [arXiv:hep-th/0407261 [hep-th]].
- [36] M. Mirzakhani, “Simple geodesics and Weil-Petersson volumes of moduli spaces of bordered Riemann surfaces,” *Invent. Math.* **167**, no.1, 179-222 (2006).
- [37] B. Eynard and N. Orantin, “Invariants of algebraic curves and topological expansion,” *Commun. Num. Theor. Phys.* **1**, 347-452 (2007) [arXiv:math-ph/0702045 [math-ph]].
- [38] B. Eynard and N. Orantin, “Weil-Petersson volume of moduli spaces, Mirzakhani’s recursion and matrix models,” [arXiv:0705.3600 [math-ph]].
- [39] P. Saad, S. H. Shenker and D. Stanford, “A semiclassical ramp in SYK and in gravity,” [arXiv:1806.06840 [hep-th]].
- [40] H. Maxfield and G. J. Turiaci, “The path integral of 3D gravity near extremality; or, JT gravity with defects as a matrix integral,” *JHEP* **01**, 118 (2021) [arXiv:2006.11317 [hep-th]].
- [41] L. V. Iliesiu, M. Mezei and G. Sárosi, “The volume of the black hole interior at late times,” *JHEP* **07**, 073 (2022) [arXiv:2107.06286 [hep-th]].
- [42] H. W. Lin, “The bulk Hilbert space of double scaled SYK,” *JHEP* **11**, 060 (2022) [arXiv:2208.07032 [hep-th]].
- [43] D. L. Jafferis, D. K. Kolchmeyer, B. Mukhametzhanov and J. Sonner, “Jackiw-Teitelboim gravity with matter, generalized eigenstate thermalization hypothesis, and random matrices,” *Phys. Rev. D* **108**, no.6, 066015 (2023) [arXiv:2209.02131 [hep-th]].
- [44] L. V. Iliesiu, A. Levine, H. W. Lin, H. Maxfield and M. Mezei, “On the non-perturbative bulk Hilbert space of JT gravity,” *JHEP* **10**, 220 (2024) [arXiv:2403.08696 [hep-th]].
- [45] J. Boruch, L. V. Iliesiu, G. Lin and C. Yan, “How the Hilbert space of two-sided black holes factorises,” *JHEP* **06**, 092 (2025) [arXiv:2406.04396 [hep-th]].
- [46] M. Miyaji, “Non-perturbative discrete spectrum of interior length and timeshift in two-sided black hole,” *JHEP* **04**, 190 (2025) [arXiv:2410.20662 [hep-th]].

- [47] D. Bak, S. H. Kim, S. Park and J. P. Song, “Machine Learns Quantum Complexity,” [arXiv:2501.02005 [quant-ph]].
- [48] M. Miyaji, S. M. Ruan, S. Shibuya and K. Yano, “Non-perturbative overlaps in JT gravity: from spectral form factor to generating functions of complexity,” JHEP **06**, 251 (2025) [arXiv:2502.12266 [hep-th]].
- [49] M. Miyaji, S. Mori and K. Okuyama, “Finite N bulk Hilbert space in ETH matrix model for double-scaled SYK. Null states, state-dependence and Krylov state complexity,” JHEP **08**, 084 (2025) [arXiv:2505.13194 [hep-th]].
- [50] C. Akers, A. Lucas and A. Vikram, “On the reconstruction map in JT gravity,” JHEP **12**, 045 (2025) [arXiv:2506.18975 [hep-th]].
- [51] V. Balasubramanian, R. N. Das, J. Erdmenger, J. Karl and H. Verlinde, “Complexity and the Hilbert space dimension of 3D gravity,” [arXiv:2602.02645 [hep-th]].
- [52] A. Bogojevic and D. Stojkovic, “A Nonsingular black hole,” Phys. Rev. D **61** (2000), 084011 [arXiv:gr-qc/9804070 [gr-qc]].
- [53] J. M. Maldacena, “Eternal black holes in anti-de Sitter,” JHEP **04**, 021 (2003) [arXiv:hep-th/0106112 [hep-th]].
- [54] A. Almheiri, T. Hartman, J. Maldacena, E. Shaghoulian and A. Tajdini, “The entropy of Hawking radiation,” Rev. Mod. Phys. **93**, no.3, 035002 (2021) [arXiv:2006.06872 [hep-th]].
- [55] I. H. Kim, E. Tang and J. Preskill, “The ghost in the radiation: robust encodings of the black hole interior (invited paper),” JHEP **06**, 031 (2020) [arXiv:2003.05451 [hep-th]].
- [56] V. Balasubramanian, A. Lawrence, J. M. Magan and M. Sasieta, “Microscopic Origin of the Entropy of Black Holes in General Relativity,” Phys. Rev. X **14**, no.1, 011024 (2024) [arXiv:2212.02447 [hep-th]].
- [57] M. Hillery, R. F. O’Connell, M. O. Scully and E. P. Wigner, “Distribution functions in physics: Fundamentals,” Phys. Rept. **106**, 121-167 (1984).
- [58] M. Brack and R. K. Bhaduri, “Semiclassical Physics,” in Frontiers in Physics, ISBN: 9780201483512, Addison-Wesley, Reading, MA, USA (1997).

- [59] P. Jizba and V. Zatloukal, “Path-integral approach to the Wigner-Kirkwood expansion,” *Phys. Rev. E* **89**, 012135 (2014) [arXiv:1309.0206 [cond-mat.stat-mech]].